Spin-Flipping Half Vortex in a Macroscopic Polariton Spinor Ring Condensate

Gangqiang Liu[1], David W. Snoke[1*], Andrew Daley[1,2], Loren Pfeiffer[3], and Kenneth West[3]
[1]*Department of Physics and Astronomy, University of Pittsburgh, Pittsburgh, PA 15260, USA*
[2]*Department of Physics and SUPA, University of Strathclyde, Glasgow G4 0NG, Scotland, UK*
[3]*Department of Electrical Engineering, Princeton University, Princeton, NJ 08544, USA*

We report the observation of vorticity in a macroscopic Bose-Einstein condensate of polaritons in a ring geometry. Because it is a spinor condensate, the elementary excitations are "half vortices" in which there is a phase rotation of π in connection with a polarization vector rotation of π around a closed path. This is clearly seen in the experimental observations of the polarization rotation around the ring. In the ring geometry, a new type of half vortex is allowed in which the handedness of the spin flips from one side of the ring to the other, in addition to the rotation of the linear polarization component; such a state is not allowed in a simply-connected geometry. Theoretical calculation of the energy of this state shows that when many-body interactions are taken into account, it is lower in energy than a simple half vortex. The direction of circulation of the flow around the ring fluctuates randomly between clockwise and counterclockwise from one shot to the next; this corresponds to spontaneous breaking of time-reversal symmetry in the system. These new, macroscopic polariton ring condensates allow for the possibility of direct control of the vorticity of the condensate.

arXiv:1402.4339v1 [cond-mat.quant-gas] 18 Feb 2014

Ring condensates, analogous to superconducting rings, have received much attention lately [1–6]; among other predictions, a ring condensate allows the possibility of macroscopic superposition states in which there is simultaneously circulation in both directions. A ring condensate is topologically distinct from a condensate in a simply connected region.

With the advance of the field of polariton condensates in the past few years, it is a natural step to create a condensate ring in a microcavity polariton system. The polariton system allows direct, nondestructive observation of the momentum distribution, energy distribution, and spatial distribution of the particles, as well as direct measurement of the coherence properties via interferometry. To make a macroscopic ring requires macroscopic transport distances as well as macroscopic coherence length. This has been achieved with polaritons, with coherent motion over tens of microns and lifetimes of 10-20 ps [7, 8], and with coherent motion of polaritons over hundreds of microns with lifetimes of 100-200 ps [9, 10].One advantage of the long-lifetime polariton systems is that the polaritons can move well away from the laser spot where they are generated, so that the laser can be viewed as a simple source term, and does not interact with the condensate. Recent work [11] has shown a very sharp transition to a trapped polariton condensate. For general reviews of previous polariton work with shorter transport distances, see Refs. 12–16.

The polaritons can be viewed as photons which have been given a small effective mass, of the order of 10^{-4} times the mass of a vacuum electron, and repulsive interactions, which are about 10^4 times stronger than the typical $\chi^{(3)}$ nonlinearities of photons in solids. The strong interactions are generated by mixing the photon states with a sharp excitonic resonance in a semiconductor inside the cavity, so that the photons pick up a fraction of the exciton-exciton interaction. Although their interactions are much stronger than typical photons in a solid medium, the polaritons are still in the weakly interacting Bose gas regime. While they have a short lifetime to remain in a cavity, after which they couple out to external photons which are detected, their lifetime is sufficient for them to interact many times with each other. In these new long-lifetime polariton systems, the ratio of lifetime in the trap to collision time is about 1000:1, comparable to the ratio for cold atom condensates.

The structure for these experiments is a planar cavity, with the mirrors made from distributed Bragg reflectors of AlAs/AlGaAs, and the exciton medium consists of GaAs/AlGaAs quantum wells embedded in this cavity. This is the same structure as that used in previous experiments, which allow coherent transport of polaritons over hundreds of microns in the two-dimensional plane of the cavity [9, 10]. The strength of the interaction between the polaritons can be tuned by varying the energy difference between the photon states and the exciton states (known as the "detuning"), which leads to a varying degree of mixing of the photons and excitons. Because the planar cavity has a wedge which gives a gradient of cavity width, we can tune the polariton-polariton interactions simply by choosing different locations on the sample with different cavity width. There is a tradeoff in how much excitonic interaction character to give to the polaritons. Less interactions (more photon-like) allows long transport length, while more interactions allows better thermalization of the polariton gas via collisions.

For these experiments we chose a region of the sample in which the polaritons were slightly more photon-like than exciton-like. We then created an in-plane harmonic potential using the inhomogeneous stress method previously demonstrated [17]. Because a shift of the exciton energy also affects the exciton-photon detuning and therefore the strength of the interaction between the polaritons, we must compensate the effect of the stress on

*email: snoke@pitt.edu

the detuning by the our initial choice of the detuning at the location in the cavity. In experiment reported here, the detuning at the location of interest was -6.7 meV without stress, and +1.9 meV with the stress applied.

We then created a Gaussian potential energy peak inside this harmonic potential using a laser focused to a spot, which generates an exciton cloud. The laser was non-resonant, with photon energy 105 meV higher than the polariton energy. This produced both excitons and polaritons at the laser focus spot. The excitons have mass four orders of magnitude larger than the polaritons, and therefore only move 1-2 μm from their point of creation; they therefore act as a static barrier for the polaritons [7–9]. The sum of the harmonic potential and the Gaussian peak due to the exciton cloud makes a Mexican-hat potential. Figure 1(a) shows our estimates for the different terms that contribute to the potential. Figure 1(b) shows the intrinsic experimental energy profile recorded using a defocused laser, and Figure 1(c) shows flow of the polaritons in the trap when the laser spot is focused, but not at the center of the trap, but instead is on the right side. The polaritons clearly flow away from the laser spot, about 35 μm, to the minimum of the harmonic potential.

To create the ring trap, we moved the laser focus to near the center of the harmonic potential minimum. As in previous work [9], when the density of the central exciton peak exceeds a critical value, there is a sharp transition to occupation of the ground state of the trap. Figure 2 shows the photon emission from the polaritons for two cases, below this critical density threshold and above the threshold. Fig. 2(a) shows the emission from the laser focus when the density is below the critical density, and Fig. 2(b) shows the filling of the ring above the critical density threshold. As seen in Fig. 2(c), the condensate is completely monoenergetic, with a very narrow spectral line width. Although there are density variations around the ring, the condensate fills in low-potential areas to maintain a single energy. This ring condensate was observed under quasi-steady state conditions, with a continuous flow of polaritons generated at the central laser spot and flowing into the ring, which replace the loss of polaritons turning into external photons outside of the cavity, while the laser is on for a duration of 25 μs. A period of 2.5 ms with the laser off between pulses was used to prevent heating of the sample.

The degree of spatial coherence of the condensate can be seen in an interference measurement. Figure 3 shows the interference pattern between two copies of the spatial image of the condensate, when one of the images is flipped $x \to -x$. There are clear fringes for the interference between one side and the other, showing that the coherence extends across the whole ring.

A closer analysis shows that the number of fringes on the top of the image in Fig. 3(a) is one more than the number of fringes on the bottom. In other words, there must be vorticity in the condensate, leading to a discontinuity in the phase. We also see stable interference patterns with one more fringe on the bottom than on the top. The pattern fluctuates from one pulse to the next, split with equal probability between these two patterns about 90% of the time, and about 10% of the time showing an equal number of fringes on the top and bottoms. We never see a difference of more than one fringe.

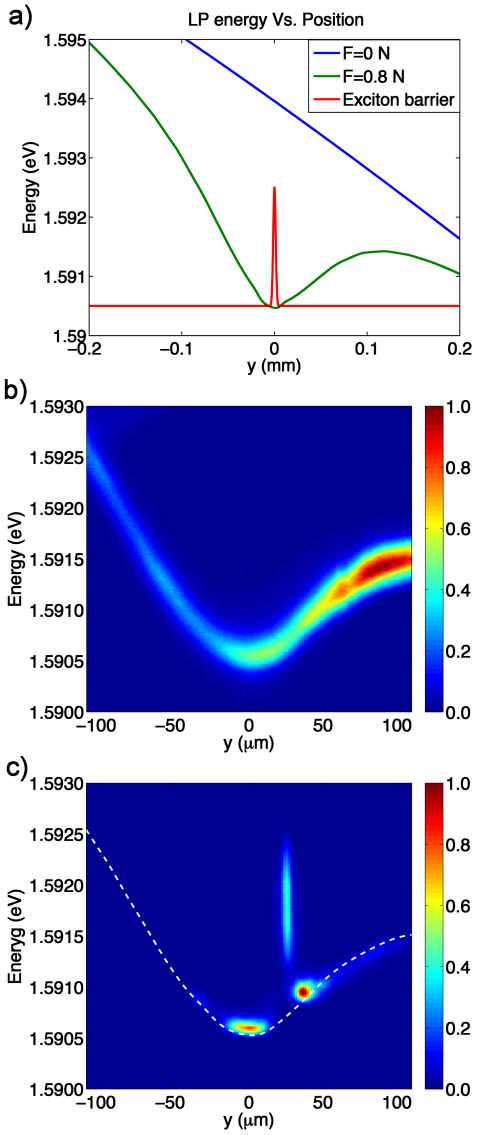

FIG. 1: a) Plot of the three terms which contribute to the potential energy felt by the polaritons. Blue line: polariton energy gradient due to the wedge in the cavity width. Green line: the energy of the polaritons shifted by inhomogeneous stress to have a harmonic potential minimum. Red line: Gaussian potential peak created by a nearly-static cloud of excitons. b) The harmonic trap and gradient potentials, seen in the photon emission spectrum from the polaritons at very low density, generated using a defocused laser. c) The same system when the laser spot is tightly focused, but set to one side instead of the center of the trap. Polaritons flow to both sides of the laser spot; some to the global minimum of the harmonic potential.

The analysis of the emission is further aided by a po-

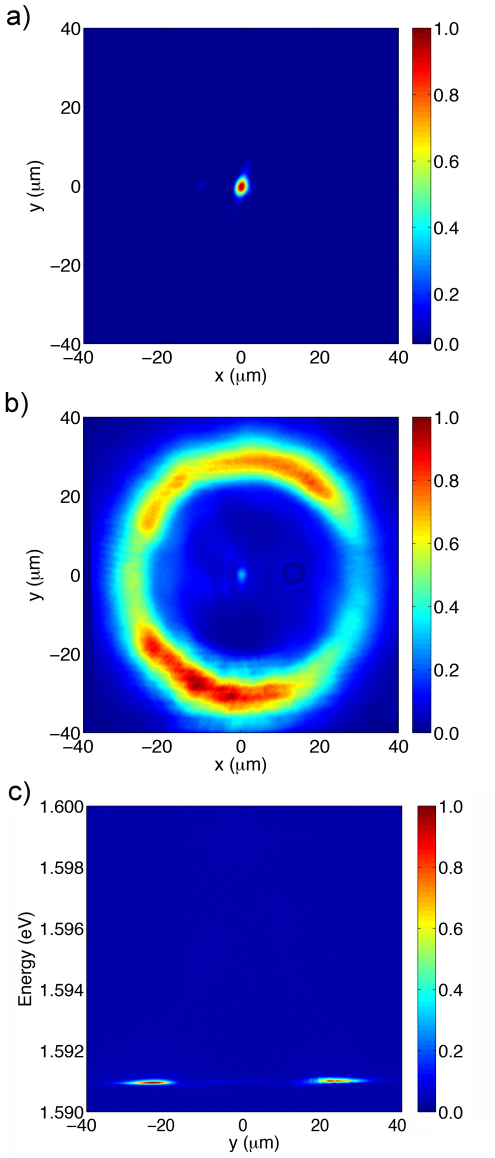

FIG. 2: a) Real-space image below critical threshold (6.7 mW cw laser power, 25 μs duration, chopped with a 1% duty cycle.) b) Real-space image well above critical threshold (300 mW cw laser power, 25 μs duration, with 1% duty cycle), c) Energy versus position along a line in the y-direction, above critical threshold, for the same conditions as (b).

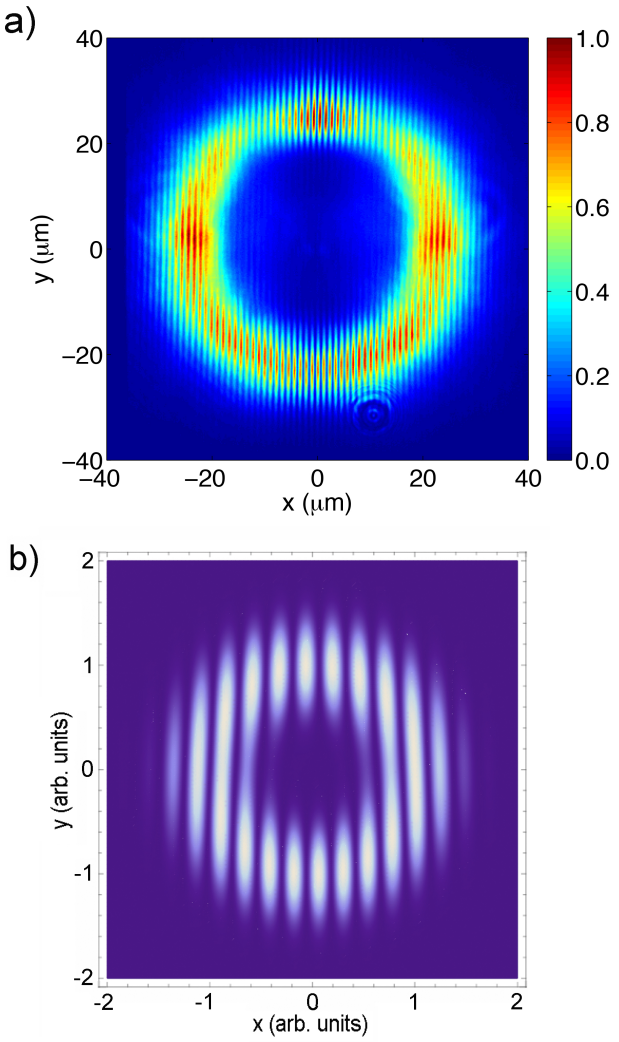

FIG. 3: a) Interference pattern between two images of the condensate, with one flipped across the y-axis, for the same conditions as Fig. 2(b) and (c). b) Theoretical prediction for the interference pattern of a half-vortex. A different angle of incidence for the two images has been chosen to give less fringes, and the thickness of the ring has been made greater, so that the overall discontinuity in the fringe pattern is easier to see.

larization analysis of the emission. Fig. 4(a) shows the direction of linear polarization at various points on the ring, deduced from measurements of the full Stokes vector of the light emitted at different points around the ring. As seen in this figure, the pattern has a 4π rotational symmetry; the linear polarization angle rotates by 180°, while the circular component flips handedness on opposite sides of the ring. This is striking given that the underlying exciton states in GaAs-based structures have a fourfold symmetry, which is seen in a fourfold symmetry of the polarization pattern under incoherent conditions [18, 19]. The orientation of the pattern is not connected to the underlying crystal symmetry; instead, it is fixed relative to the gradient of potential which exists in the system, which comes from the wedge in the cavity width. The polarization pattern also does not depend on the polarization of the laser which generates the polaritons at the central spot.

The interference pattern and the polarization measurements can both be understood as the effects of a quantum half vortex. This effect, which has also been predicted for spinor atom condensates [20] and d-wave superconductors [21] has been analyzed for polaritons by Y. Rubo [22], and has been reported experimentally for a polariton condensate localized in a sub-micron disorder minimum [23, 24]. However, the state we see here is distinct from

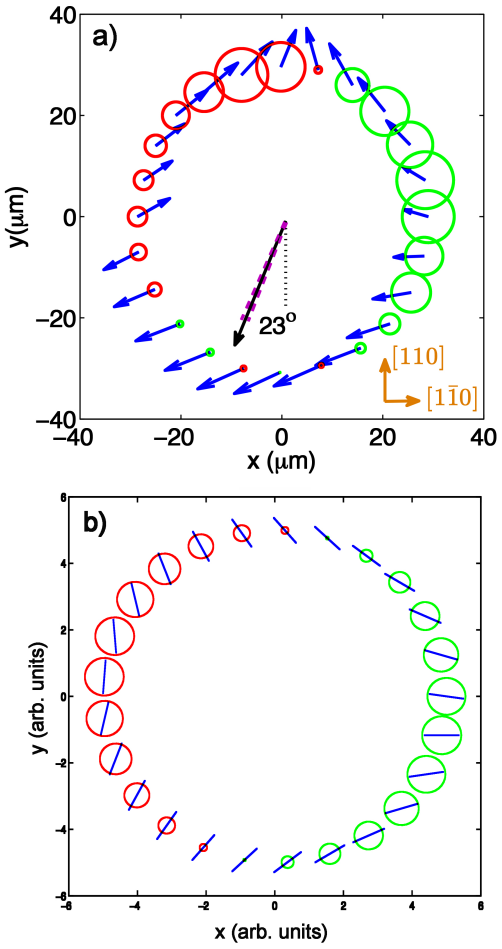

FIG. 4: a) Experimental results for the polarization of the light emission from the ring at various positions. The length of the arrows is proportional to the degree of linear polarization, and the radius of the circles is proportional to the degree of circular polarization (green: right-handed; red: left-handed). The arrow marked with purple shows the direction of the overall gradient of the cavity, which gives a local maximum of the polariton density in both regions where the circular polarization drops to zero. b) Theoretical polarization pattern for the condensate wave function given by (3), with $k = m = -1/2$ and $f = -0.3$.

the standard half vortex state, because we have a ring geometry instead of a simply connected geometry.

A half vortex can be thought of as a π rotation in phase around a closed path accompanied by a π rotation of the polarization angle. In terms of the linear polarization components in the plane of the sample, we can write the elementary half-vortices as

$$\vec{\varphi}_{k,m}(\theta) = \sqrt{n(\theta)}e^{im\theta}\left[f\begin{pmatrix}\cos(k\theta)\\ \sin(k\theta)\end{pmatrix} - i\,\mathrm{sgn}(km)\sqrt{1-f^2}\begin{pmatrix}\sin(k\theta)\\ -\cos(k\theta)\end{pmatrix}\right]. \quad (1)$$

Here, $m, k \in \{-1/2, +1/2\}$ select the rotation directions for the phase and polarization of the half-vortex, respectively; $n(\theta)$ is the effective one-dimensional density of the condensate, and f is a real constant, with $|f| \leq 1$. For each combination of k and m, this ansatz describes a half-vortex with constant degree of circular polarization $c = \mathrm{sgn}(km)2f\sqrt{1-f^2}$, and a linear phase angle that (for $|f| \neq 1/\sqrt{2}$) rotates as $k\theta$. In the absence of interactions, and in a homogeneous ring $n(\theta) = n$, these states with $|f| = 1/\sqrt{2}$ are eigenstates of the Hamiltonian, which consists only of the kinetic energy,

$$H_{\mathrm{kin}} = -\frac{\hbar^2}{2m}\nabla^2 \equiv -\frac{\hbar^2}{2mR^2}\frac{d^2}{d\theta^2}, \quad (2)$$

where m is the effective mass of the polaritons.

In a simply connected geometry, only half vortices of this type are allowed, because there is a boundary condition that the circular polarization must be continuous at $r = 0$. However, in a ring geometry, this condition is relaxed, and other wave functions with half vorticity also satisfy the condition that the wave function be single-valued. The experimentally observed polarization pattern is reproduced by using the following form for the half vortices:

$$\vec{\psi}_{k,m}(\theta) = \sqrt{n(\theta)}e^{im\theta}\left[f\begin{pmatrix}\cos(k\theta)\\ \sin(k\theta)\end{pmatrix} + i\,\mathrm{sgn}(km)\sqrt{1-f^2}\begin{pmatrix}\sin(k\theta)\\ \cos(k\theta)\end{pmatrix}\right]. \quad (3)$$

This gives the polarization map shown in Fig. 4(b). It provides a half-vortex with a phase rotation direction chosen by the sign of m. For these states, the degree of circular polarization is given by $c = -\,\mathrm{sgn}(km)2f\sqrt{1-f^2}\cos(2k\theta)$, so that the circular polarization direction, i.e., the z-component of the spin-1 particles, flips from one side of the ring to the other, as seen in the experimental data of Fig. 4(a). The linear polarization angle is given by

$$\frac{1}{2}\arg\left(\frac{f + \mathrm{sgn}(km)\sqrt{1-f^2}\,e^{2ik\theta}}{f\,e^{2ik\theta} - \mathrm{sgn}(km)\sqrt{1-f^2}}\right), \quad (4)$$

which can rotate in either direction, and this direction is determined by the sign of k in the ansatz. Note that any sign of k and m can be paired here.

The $x \to -x$ interference pattern for the wave function (3) is shown in Fig. 3(b) (for details, see the online supplementary information). As seen in this figure, it reproduces the observation of a difference of one between the top and bottom of the pattern; a full vortex would give a difference of two fringes between the top or the bottom. This is different from the case of interference of a vortex state with a plane wave, which would give a difference of one fringe for a full vortex, and a difference of one fringe in one of the two circular polarizations for a half vortex.

When we use the experimentally measured density variation $n(\theta)$ around the ring, which is proportional to

the intensity of the light emitted at each point, we find that the ansatz (3) has lower energy than the elementary half vortex states, and lower energy than a full vortex. We evaluate the energy using a variational approach in an effective 1D model, determining f by minimizing the total energy $E = E_{\rm kin} + E_{\rm int}$, consisting of the kinetic energy

$$E_{\rm kin} = \frac{1}{2\pi}\int_0^{2\pi} d\theta \vec{\psi}^*(\theta)\cdot\left[-\frac{\hbar^2}{2mR^2}\frac{d^2}{d\theta^2}\right]\vec{\psi}(\theta) \qquad (5)$$

and the interaction energy [22]

$$E_{\rm int} = \frac{1}{4\pi}\int_0^{2\pi} d\theta \left[(U_0-U_1)(\vec{\psi}^*\cdot\vec{\psi})^2 + U_1|\vec{\psi}^*\times\vec{\psi}|^2\right]. \qquad (6)$$

Here, U_0 and U_1 are the interaction constants, which can be written in terms of the interactions between the same circular polarisation $M_{\uparrow\uparrow}$ and different circular polarisations $M_{\uparrow\downarrow}$, as $U_0 = M_{\uparrow\uparrow}$, U_1=$M_{\uparrow\uparrow} - M_{\uparrow\downarrow}$. Relative to $M_{\uparrow\uparrow}$, $M_{\uparrow\downarrow}$ is small and is attractive rather than repulsive. In our numerical calculations, we take $M_{\uparrow\downarrow}/M_{\uparrow\uparrow} \approx -0.05$.

In the presence of interactions, even in a homogeneous ring, the degree of circular polarization is fixed by the competition between interaction energy and kinetic energy. For smaller ring radius R, greater degree of circular polarization is favored by the kinetic energy, but stronger interactions favor greater linear polarization. Therefore a higher polariton density will lead to a smaller degree of circular polarization and $|f| \neq 1/\sqrt{2}$. Since the density of the condensate in our experiments varies around the ring, with maxima on opposite sides of the ring in the direction of the overall cavity gradient, this favors a separation into linear polarization at the regions of high density and circular polarization in between, as seen in the polarization map.

The theoretical analysis we have done shows that the pattern of varying linear and circular polarization around the ring, with orthogonal polarizations on opposite sides the ring, is to be expected for the density variation around the ring in these experiments. However, the theory does not explain the particular choice of direction of linear polarization seen at the region of highest density or the particular choice split of right- and left-handedness of the circular polarization seen on the sides of the ring. The underlying four-fold symmetry of the GaAs may play a role, but when when we put into the Hamiltonian the energy for the splitting of the polarization states, which is known [18, 19] to give energy splittings of order 100 μeV, it does not make a significant contribution to the energy of the half vortex states.

Future theoretical work should include terms for the generation and decay of the polaritons, to explore why the condensate is preferentially in this spin-flipping half vortex state, rather than the ground state with no circulation. Under some circumstances, the no-vortex state can be unstable when generation and decay are accounted for [25]. Further experimental work can use a resonant laser beam to inject angular momentum unto the condensate; that is, to stir it. In this case, we may see states which are a superposition of left and right circulation, as are seen in superconducting rings at the point of a half quantum of magnetic flux. We also have the possibilities of stabilizing the circulation to go in only one direction, and introducing small barriers in the ring using a laser-generated exciton cloud, to create Josephson junctions. Since we can observe the interference patterns directly from the light leaking through the mirrors, we can non-destructively measure the phase map for all the states we produce.

As we have seen, the polarization rotation is pinned in this system while the direction of circulation of current around the ring is not. The laser focused at the center of the ring does not introduce any circulation. As a result, we see a random occurrence of circulation to the left or right, even as the polarization is pinned. These experimental results can therefore be seen as an example of spontaneous time-reversal symmetry breaking leading to a persistent current around the ring, with a phase coherence time at least a hundred thousand times longer than the lifetime of any one particle in the condensate.

Because we have a macroscopic ring geometry which is topologically distinct from a simply-connected geometry, we see a different topology of the vortex, with the spin of the particles flipping around the ring, even as they remain in a single, macroscopic wave function. The spin-flipping half vortex cannot be continuously transformed into a standard half vortex. The vortex seen here is different from the typical case of pairs of vortices of opposite vorticity generated due to turbulence [26, 27], and also can be produced on demand, as opposed to needing to search for a pinned vortex at a random location in a disordered landscape, as was the case for Ref. [23].

Acknowledgements. This work has been supported by the National Science Foundation under grant DMR-1104383. The work at Princeton was partially funded by the Gordon and Betty Moore Foundation as well as the National Science Foundation MRSEC Program through the Princeton Center for Complex Materials (DMR-0819860).

[1] C. Ryu, P. W. Blackburn, A. A. Blinova, and M. G. Boshier, Phys. Rev. Lett. **111**, 205301 (2013); C. Ryu, M. F. Andersen, P. Cladé, V. Natarajan, K. Helmerson, and W. D. Phillips, Phys. Rev. Lett. **99**, 260401 (2007). M. F. Andersen, C. Ryu, Pierre Cladé, V. Natarajan, A. Vaziri, K. Helmerson, and W. D. Phillips, Phys. Rev. Lett. **97**, 170406 (2006).

[2] A. Ramanathan, K. C. Wright, S. R. Muniz, M. Zelan, W. T. Hill, III, C. J. Lobb, K. Helmerson, W. D. Phillips, and G. K. Campbell, Phys. Rev. Lett. **106**, 130401 (2011).

[3] K. C. Wright, R. B. Blakestad, C. J. Lobb, W. D. Phillips, and G. K. Campbell, Phys. Rev. Lett. **110**, 025302 (2013).

[4] S. Beattie, S. Moulder, R.J. Fletcher, and Z. Hadzibabic, Phys. Rev. Lett. **110**, 025301 (2013).

[5] D.W. Hallwood, K. Burnett, and J. Dunningham, New J. Phys. **8**, 180 (2006); D.W. Hallwood and J. Brand, Phys. Rev. A **84**, 043620 (2011).

[6] R. Kanamoto and E.M. Wright, J. Optics **13**, 064011 (2011).

[7] E. Wertz, L. Ferrier, D. D. Solnyshkov, R. Johne, D. Sanvitto, A. Lemaître, I. Sagnes, R. Grousson, A. V. Kavokin, P. Senellart, G. Malpuech, and J. Bloch Nature Phys. **6**, 860 (2010).

[8] P. Cristofolini, A. Dreismann, G. Christmann, G. Franchetti, N.G. Berloff, P. Tsotsis, Z. Hatzopoulos, P. G. Savvidis, and J. J. Baumberg Phys. Rev. Lett. **110**, 186403 (2013).

[9] B. Nelsen, G. Liu, M. Steger, D.W. Snoke, R. Balili, K. West and L. Pfeiffer, Phys. Rev. X **3**, 041015 (2013).

[10] M. Steger, G. Liu, B. Nelsen, C. Gautham, D.W. Snoke, R. Balili, L. Pfeiffer and K. West Phys. Rev. B **88**, 235314 (2013).

[11] P. Wen, Y. Sun, K.A. Nelson, B. Nelsen, G. Liu, M. Steger, D.W. Snoke, L.N. Pfeiffer, and K. West, "Phase Diagram of Bose-Einstein Condensation of Long-Lifetime Polaritons in Equilibrium," under review.

[12] A. Kavokin, J.J. Baumberg, G. Malpuech, and F.P. Laussy, *Microcavities*, (Oxford University Press, 2011).

[13] D.W. Snoke, in *Exciton Polaritons in Microcavities* (Springer Series in Solid State Sciences **172**), V. Timofeev and D. Sanvitto, eds. (Springer, 2012).

[14] H. Deng, H. Haug, and Y. Yamamoto, Rev. Modern Phys. **82**, 1489 (2010).

[15] I. Carusotto and C. Ciuti, Rev. Modern Phys. **85**, 299 (2013).

[16] David Snoke and Peter Littlewood, Physics Today **63**, 42 (2010).

[17] R. Balili, D. Snoke, L. Pfeiffer, and K. West, Applied Phys. Lett. **88**, 031110 (2006).

[18] N.W. Sinclair, J.K. Wuenschell, Z.Vörös, B. Nelsen, D. W. Snoke, M. H. Szymanska, A. Chin, J. Keeling, L.N. Pfeiffer and K.W. West, Phys. Rev. B **83**, 245304 (2011).

[19] R. Balili, B. Nelsen, D.W. Snoke, R.H. Reid, L. Pfeiffer, and K. West, Physical Review B **81**, 125311 (2010).

[20] S. Sinha, R. Nath, and L. Santos, Phys. Rev. Lett. **107** , 270401 (2011).

[21] M. Machida, T. Koyama, and M. Kato, and T. Ishida, Physica C **412**, 367 (2004).

[22] Y.G. Rubo, Phys. Rev. Lett. **99**, 106401 (2007).

[23] K. G. Lagoudakis, T. Ostatnický, A. V. Kavokin, Y. G. Rubo, R. André, and B. Deveaud-Plédran, Science **326**, 974 (2009).

[24] F. Manni, K.G. Lagoudakis, T.C.H. Liew, R. André, V. Savona, and B. Deveaud, Nature Comm. **3**, 1309 (2012).

[25] J. Keeling and N.G. Berloff, Phys. Rev. Lett. **100**, 250401 (2008).

[26] F. Manni, T.C.H. Liew, K.G. Lagoudakis, C. Ouellet-Plamondon, R. André, V. Savona, V, and B. Deveaud, Phys. Rev. B **88**, 201303 (2013).

[27] G. Tosi, F.M. Marchetti, D. Sanvitto, C. Anton, M.H. Szymanska, A.Berceanu, C. Tejedor, L. Marrucci, A. Lemaitre, and J. Bloch, Phys. Rev. Lett. **107**, 036401 (2011).